

1 Model for artificial ionospheric duct formation due to HF heating

2 G. M. Milikh,¹ A. G. Demekhov,² K. Papadopoulos,¹ A. Vartanyan,¹ J. D. Huba,³
 3 and G. Joyce⁴

4 Received 28 January 2010; revised 22 February 2010; accepted 26 February 2010; published XX Month 2010.

5 [1] Strong electron heating by the injection of highly
 6 powerful HF waves can lead to the formation of
 7 ionospheric plasma density perturbations that stretch along
 8 the magnetic field lines. Those density perturbations can
 9 serve as ducts for guiding natural and artificial ELF/VLF
 10 waves. This paper presents a theoretical model of duct
 11 formation due to HF heating of the ionosphere. The model
 12 is based on the modified SAMI2 code, and is validated by
 13 comparison with two well documented experiments. One
 14 experiment, conducted at the SURA heating facility, used
 15 the low orbit satellite DEMETER as a diagnostic tool to
 16 measure the electron and ion temperature and density along
 17 the overflying satellite orbit close to the magnetic zenith of
 18 the HF-heater. The second experiment, conducted at the
 19 EISCAT HF facility and diagnosed by the EISCAT
 20 Incoherent Scatter Radar, measured the vertical profiles of
 21 the electron and ion temperature between 150–600 km. The
 22 model agrees well with the observations, and provides a
 23 new understanding of the processes during ionospheric
 24 modification. **Citation:** Milikh, G. M., A. G. Demekhov,
 25 K. Papadopoulos, A. Vartanyan, J. D. Huba, and G. Joyce (2010),
 26 Model for artificial ionospheric duct formation due to HF heating,
 27 *Geophys. Res. Lett.*, 37, LXXXXX, doi:10.1029/2010GL042684.

28 1. Introduction

29 [2] It is well known that the presence of field aligned
 30 density structures plays a critical role in the propagation of
 31 whistler waves in the ionosphere. The density structures
 32 serve as ducts for VLF/ELF waves since the density gradient
 33 perpendicular to the magnetic field can lead to their total
 34 internal reflection [*Streltsov et al.*, 2006]. Such density
 35 structures have often been observed [*Carpenter et al.*, 2002]
 36 to extend over distances covering entire magnetic field lines.
 37 They are known to trap and guide whistler-mode waves
 38 between conjugate regions [e.g., *Koons*, 1989].

39 [3] The possibility for creating such trans-hemispheric
 40 ducts artificially was discussed by *Perrine et al.* [2006],
 41 where a 1D model which simulates the plasma along an
 42 entire magnetic dipole field line was used. It was shown that
 43 long term continuous HF heating of the F-region by powerful
 44 ionospheric heaters, such as HAARP, generates a strong
 45 thermal wave in the ionospheric and magnetospheric plasma.
 46 The thermal wave propagates along the magnetic field line

through the topside ionosphere and magnetosphere, driving
 ion outflows, displacing the ambient plasma and leading to
 the formation of density ducts that stretch along the mag-
 netic field line to the conjugate point. We have recently
 generalized the previous 1D computational model to a 2D
 model by incorporating simulations of the plasma in the
 latitudinal direction. The new model allows one to describe
 the ionospheric parameters in both vertical and latitudinal
 directions with much better resolution than the old one.
 Therefore the new model allows for close and useful com-
 parisons with data obtained by radars and satellites that the
 old model does not allow. The key objective of this paper is
 to validate this new model based on SAMI2. To accomplish
 this we will check the model against two recent well diag-
 nosed experiments which detected large scale ducts caused
 by the HF heating. One experiment was conducted at the
 SURA heating facility and used the low orbit satellite
 DEMETER [*Berthelier et al.*, 2006a, 2006b] as a diagnostic
 tool [*Frolov et al.*, 2008] to measure the electron and ion
 temperature and density along the satellite orbit close to the
 magnetic zenith of the HF-heater. Another heating experi-
 ment, conducted at the EISCAT HF facility and diagnosed
 by the EISCAT Incoherent Scatter Radar (ISR) [*Rietveld et*
al., 2003], measured the vertical profiles of the electron and
 ion temperature between 150–600 km.

[4] The letter is organized as following: the next section
 describes the numerical model applied. In the discussion
 section the model output is compared with the EISCAT radar
 and DEMETER observations followed by conclusions.

2. Numerical Model of Formation of the Artificial Ducts

[5] The theoretical/computational model is based on the
 SAMI2 code developed at the Naval Research Laboratory
 [*Huba et al.*, 2000]. The code is a Eulerian grid-based code,
 which describes an ionosphere made up of seven ion species.
 The equations of continuity and momentum are solved for
 the electrons and each ion species, with the temperature
 equation solved for the electrons and H⁺, He⁺, and O⁺
 species. The electron density is determined on the basis of
 charge neutrality. The code includes $E \times B$ drift of the field
 lines with frozen-in plasma (in altitude and longitude), an
 empirical neutral atmosphere model, horizontal winds,
 photo-deposition into the ionosphere, ion chemistry models,
 and ion inertia. This inclusion of ion inertia is critical since it
 allows for the study of sound wave propagation in the
 plasma. The SAMI2 model is inter-hemispheric and can
 simulate the plasma along the entire dipole magnetic field line
 (for the geometry of the model see *Perrine et al.* [2006]). The
 most recent version of the SAMI2 code (release 0.98) which
 allows description of processes at high latitudes was used
 here. HF heating of the ionosphere is a complex phenomenon.

¹Department of Physics and Department of Astronomy, University of Maryland, College Park, Maryland, USA.

²Institute of Applied Physics, Russian Academy of Sciences, Nizhny Novgorod, Russia.

³Naval Research Laboratory, Washington, DC, USA.

⁴Icarus Research, Inc., Bethesda, Maryland, USA.

106 It begins with the HF absorption which pumps the iono-
 107 spheric turbulence that in turn generates the plasma heating
 108 [Gurevich *et al.*, 1996; Gustavsson *et al.*, 2001]. Since the
 109 SAMI2 code does not consider wave propagation and ab-
 110 sorption we introduced in the model a flexible source of
 111 electron heating, as we did it in an earlier paper by Perrine *et*
 112 *al.* [2006]. This source of the electron heating was presented
 113 in the form of localized heating rate per electron

$$q = \frac{\mu P}{V n_e} f(x, z) = 260 \mu P (MW) \left(\frac{10 km}{a} \right) \left(\frac{300 km}{z_{up}} \right)^2 \cdot \frac{1}{\tan^2 \Theta} f(x, z) K/s \quad (1)$$

114 Here P is the power of the HF heater, V is the volume of the
 115 HF absorbed region, n_e is the electron density in this region,
 116 while μ is the absorption efficiency. $f(x, z)$ describes the
 117 spatial distribution of the HF beam power density taken as

$$f(x, z) = e^{-(z-z_{up})^2/a^2} e^{-\ln 2 [(x-x_0)^2/b^2]} \quad (2)$$

118 The center of the heated region is taken at the upper hybrid
 119 altitude z_{up} . Furthermore, b is the half-power beam width near
 120 the upper hybrid point. The HF-irradiated spot is taken as a
 121 circle centered at x_0 having the angular half-widths Θ so that
 122 $b = z_{up} \tan \theta$, and the HF-irradiated volume is $V = \pi a b^2$.
 123 Finally, it is assumed that electron heating occurs in an al-
 124 titude range having the vertical extent a between the wave
 125 reflection point and the upper hybrid height, which is
 126 dominated by the anomalous absorption [Gurevich *et al.*,
 127 1996].

128 [6] In this paper we will model the ionospheric conditions
 129 at Tromso during 10/07/99 at the time of the EISCAT
 130 experiment [Rietveld *et al.*, 2003]. We therefore use in the
 131 SAMI2 code the corresponding A_p and $F_{10.7}$ indexes, and
 132 assume that the heating began 10/7/99 at 19:24 UT. The
 133 radiated HF power was 960 kW, the half power beam
 134 width was 12° , and the facility was operated at a frequency
 135 of 4.5 MHz. Furthermore, for the unperturbed profile of
 136 the electron density we find that the reflection height for
 137 the 4.5 MHz frequency is located at 280 km, while the
 138 upper hybrid height is at about 10 km below. Thus the
 139 vertical extent of the anomalous absorption region is taken
 140 as $a = 10$ km.

141 [7] Before proceeding we should caution the reader on the
 142 timescale of model validity. The model neglects the hori-
 143 zontal transport caused by the $\mathbf{E} \times \mathbf{B}$ drift, which has a time
 144 scale $t_{dr} = b/v_{dr}$, where v_{dr} is the drift velocity and b is the
 145 horizontal scale of the heated region. Taking into account
 146 that the Tromso HF-heater has a half-power beam width of
 147 12° and that the electron heating occurs at an altitude of
 148 300 km, we obtain that the horizontal scale of the heated
 149 region is $b = 60$ km. Moreover during the time of the dis-
 150 cussed experiments the detected drift velocity was 200–
 151 300 m/s [Rietveld *et al.*, 2003]. Thus the $\mathbf{E} \times \mathbf{B}$ drift led to
 152 energy loss followed by the reduction of the heating effect
 153 on a time scale of 3.5–5.0 minutes.

154 2.1. Simulation Procedure

155 [8] The code starts up from empirically determined initial
 156 conditions 24 hours before the specific heating time, and
 157 runs for 24 hours of ‘world clock time’. This practice allows
 158 the system to relax to ambient conditions, and reduces noise

in the system due to the initialization. Furthermore, the
 neutral density model was adjusted so that the computed
 f_0F_2 peak matched the observed. Then the ‘‘artificial heater’’
 turns on and begins to pump energy into the electrons, using
 the specified parameters for that run. Artificial heating
 continues for some time continuously pumping energy into
 the electrons at the specified altitude, and the perturbations
 in ion and electron properties are tracked as they travel
 along the field line. Then the heater switches off, allowing
 the ionosphere to relax back to ambient conditions. The
 latter may also vary according to the natural factors which
 determine the ionosphere dynamics. This procedure mini-
 mizes noise due to the initialization and allows for the
 perturbations in the ionosphere to travel along the field lines,
 and the ionosphere to relax following strong heating. It
 describes the plasma response to the removal of the artificial
 heating as well as to its application.

[9] In order to isolate and measure the perturbations
 directly, a duplicate set of runs was made, identical to the
 run described, but with a different heating rate defined by
 factor q in equation (1). In addition, one run without arti-
 ficial heating was performed. We refer to this as ‘‘ambient’’
 or ‘‘reference’’ run, while those with artificial heating are
 ‘‘heated’’ runs. The ionosphere changes during a simulation
 due to natural causes, so the perturbations in the heated runs
 due to artificial heating would not be easily identifiable on
 their own. But since the same natural variations are present
 in the ambient data, scaling (or subtracting) by the ambient
 data provides a simple way to decouple the natural varia-
 tions from the heater induced perturbations.

3. Discussion

3.1. Comparison With Tromso Experiments

[10] In order to reproduce results of the ISR observations
 made at Tromso we conducted some runs using the speci-
 fied conditions at Tromso 10/7/99. Namely, we considered
 the index $A_p = 5$, and that the HF heating began at 19:24 UT.
 For the specified heater and antenna characteristics at
 EISCAT equation (1) gives that $q = 12,400 \mu$, K/s. In our
 runs the heating rate varied in the range 2,000–8,000 K/s
 which corresponds to the absorption efficiency $\mu = 0.16$ –
 0.64. Note that Gustavsson *et al.* [2001] used the radar
 data collected during the heating experiments at Tromso to
 estimate the heating rate per electron as 3,000 K/s. This
 value corresponds to the absorption efficiency $\mu = 0.25$,
 which is within the range of our estimates.

[11] Figure 1 shows the height profile of the electron
 density normalized to its ambient value computed at dif-
 ferent times for a given pumping rate $q = 8,000$ K/s which
 corresponds to an absorption efficiency $\mu = 0.64$. The
 heating was switched on at 19:24:00 UT for 8 minutes. The
 traces labeled 1 to 3 correspond to times separated by
 3 minutes starting at 19:25:46, i.e. 1 min and 46 s into the
 heating. The trace 4 corresponds to cooling over 2 minutes
 and 49 seconds. Figure 1 reveals that the electron heating
 increases the plasma pressure and thus pushes the plasma
 from the heated region along the magnetic field line. Con-
 sequently, the plasma density in the heated region drops by
 more than 20%, but on a timescale larger than 5 minutes, as
 shown by the trace 3.

[12] Figure 2 shows the results of our model super-
 imposed onto the observation results presented by Rietveld

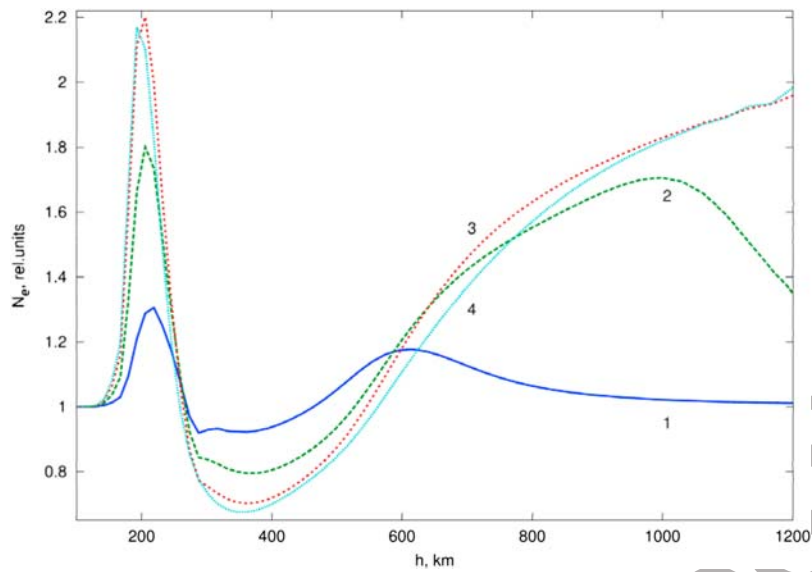


Figure 1. The electron density normalized to its ambient value computed at different times for a pumping rate $q = 8,000$ K/s which corresponds to the absorption efficiency $\mu = 0.64$. The heating was switched on at 19:24:00 UT for 8 minutes. The traces labeled 1 to 3 correspond to times separated by 3 minutes starting at 19:25:46, i.e. 1 min and 46 s into the heating. The trace 4 corresponds to cooling over 2 minutes and 49 seconds.

220 *et al.* [2003, Figure 3]. The latter were made by the EISCAT
 221 ISR at 19:28 UT. Figure 2 (left) shows the observed altitude
 222 profile of the electron density (circles) and that computed by
 223 the SAMI2 model (continuous trace) for 4 minutes in the
 224 heating. Figure 2 (middle) shows the observed ion temper-

ature (circles) and electron temperature (crosses) along with
 the three traces generated by SAMI2 model.

[13] In order to improve agreement between the model
 and observations the neutral density in the model was
 adjusted so that the computed f_oF_2 peak matches the ob-

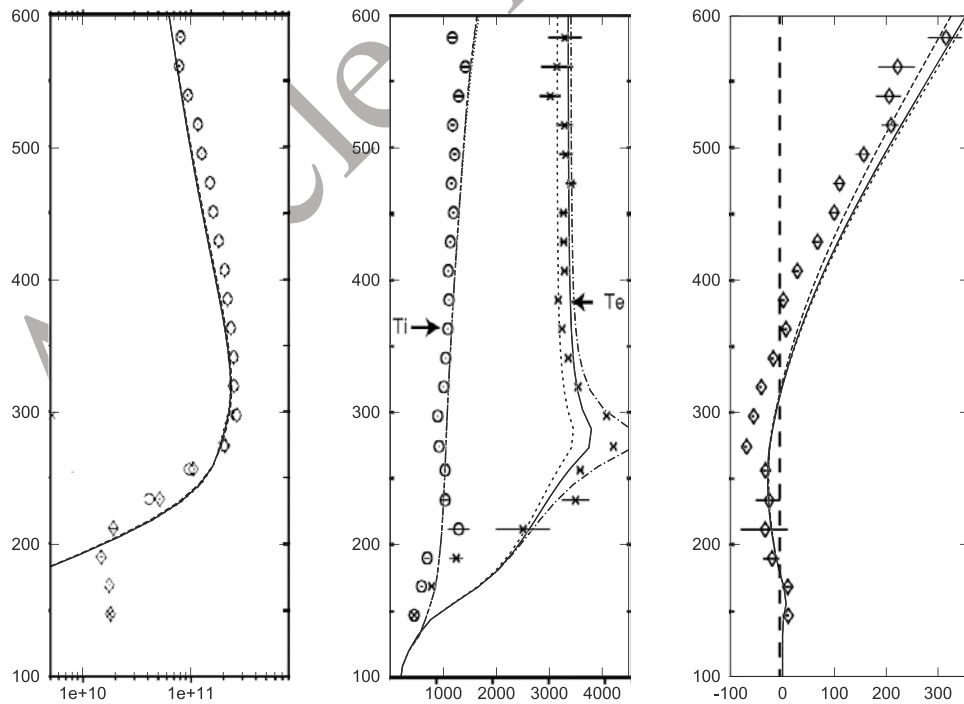


Figure 2. (left) The observed altitude profile of the electron density (circles) and the one computed by SAMI2 (continuous trace) for the four minute time interval starting on at 10/07/99 at 19:24:00 UT. (middle) The observed ion temperature (circles) and electron temperature (crosses) along with the three traces generated by the SAMI2 model. The dashed, solid, and dot-dashed line corresponds to the absorption efficiencies $\mu = 0.16, 0.32$ and 0.64 respectively. (right) The observed ion velocity (diamonds) along with the three traces which correspond to the computations made at $\mu = 0.16, 0.32$ and 0.64 (from left to right).

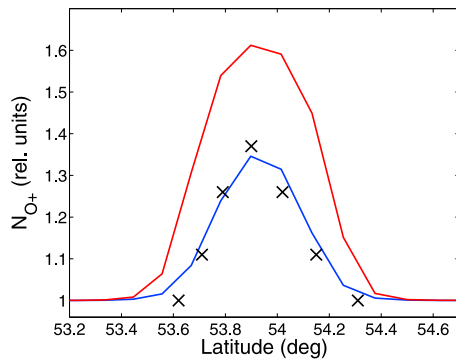


Figure 3. Relative changes in the density of O^+ ions computed for the two different absorption efficiencies $\mu = 0.17$ and 0.29 . The crosses show DEMETER observations reported by Frolov *et al.* [2008].

230 servations. For this purpose we have reduced the density of
 231 the atomic oxygen in the model by 50%. Such an approach is
 232 justified by the fact that SAMI2 uses averaged model values
 233 of the neutral density which may not very accurate. The
 234 adjustment leads to significant changes in the electron
 235 temperature and affects the vertical velocity only slightly.
 236 The dashed, solid, and dot-dashed lines in Figure 2 cor-
 237 responds to the absorption efficiencies $\mu = 0.16, 0.32$ and
 238 0.64 , respectively. Note that the changes in μ affect only
 239 the values of electron temperature, while the ion temper-
 240 ature remains unperturbed during a relatively short heating
 241 pulse. Figure 2 (right) shows the observation of the ion
 242 velocity (diamonds) along with the three traces which
 243 correspond to the computations made at different absorp-
 244 tion efficiencies $\mu = 0.16, 0.32$ and 0.64 (from the left to
 245 right). Also, in this case the HF heating duration did not
 246 exceed the time scale of $E \times B$ drift and thus the energy
 247 loss due to horizontal transport can be neglected.

248 [14] Figure 2 reveals that (1) HF heating with the absorp-
 249 tion efficiencies $\mu = 0.3-0.6$ drives perturbations of the
 250 electron temperature in good agreement with those detected
 251 by the ISR and (2) The computed ion velocity fits well with
 252 the observations. Namely, it shows that the ion velocity is
 253 negative below the heating region, and positive above it. A
 254 strong electron heating increases the electron pressure and
 255 pushes the plasma both down and upward from the heated
 256 region. Thus below this region the ion velocity is negative
 257 (downward directed), while above the region it is positive
 258 (upward directed) and its value increases with altitude
 259 since the plasma propagates in the ionosphere of decreas-
 260 ing density.

261 3.2. Comparison With SURA Experiments

262 [15] Frolov *et al.* [2008] reported the detection of plasma
 263 ducts by the DEMETER satellite overflying the SURA HF-
 264 heater. In fact, ducts were detected when the heater operated
 265 at 4.3 MHz, and at ERP = 80 MW, while the half-power
 266 beam width was 12° on 05/01/06. The ionosphere was quiet,
 267 $K_p = 0$, and the heating wave was reflected at 230 km,
 268 below the f_oF_2 peak.

269 [16] We conducted SAMI2 runs for this day for SURA
 270 location ($56^\circ N, 46^\circ E$) using the specified characteristics
 271 of the HF-heater. The heating began 10 minutes before
 272 the DEMETER overfly at 18:28:39 UT, and lasted for

15 minutes. Figure 3 shows the relative changes in the
 density of O^+ ions computed for the two different pumping
 rates $q = 1,000$ and $1,700$ K/s which correspond to the
 absorption efficiency $\mu = 0.17$ and 0.29 respectively. The
 increase in O^+ density was then checked against the
 DEMETER observations shown by crosses. The latter data
 were derived from the DEMETER observations of the time
 series of O^+ density [Frolov *et al.*, 2008]. We converted
 these data into the relative ion density by dividing them by
 the value of the unperturbed O^+ density measured outside the
 duct. In addition, we presented the relative O^+ density as a
 function of latitude by taking into account the orbital velocity
 $v = 7$ km/s of DEMETER. Figure 3 shows a good agreement
 between the observations and model for the case of the
 absorption efficiency $\mu = 0.17$. Note that similar HF heating
 experiments were conducted at HAARP using Demeter as a
 diagnostic tool [Milikh *et al.*, 2008].

3.3. Concluding Remarks

[17] Recently modified SAMI2 numerical model was val-
 idated by comparison with two well documented experi-
 ments. One experiment, conducted at the SURA heating
 facility, used the low orbit satellite DEMETER as a diag-
 nostic tool to measure the electron and ion temperature and
 density along the overflying satellite orbit close to the
 magnetic zenith of the HF-heater. The second experiment,
 conducted at the EISCAT HF facility and diagnosed by the
 EISCAT ISR, measured the vertical profiles of the electron
 and ion temperature between 150–600 km. The model
 reproduces the observations with high accuracy, which
 indicates its potential as a key tool for study of the arti-
 ficial ducts, and to guide future observational campaigns. In
 addition, the model predicts that the ionospheric HF heating
 could produce strong perturbations of the plasma pressure
 which will then transform into magnetic field perturbations
 that could be detected by low orbit satellites having on-board
 magnetometers such as DMSP. Moreover by checking the
 model results against the ISR or satellite made observations
 one can assess efficiency of the duct production, namely what
 fraction of the radio beam energy was pumped into the ducts.

[18] **Acknowledgments.** The work was supported by DARPA via a
 subcontract N684228 with BAE Systems. It was also supported by the
 ONR grant NAVY.N0017302C60 and by the ONR MURI grant
 N000140710789. The work of A.D. was also supported in part by the Russian
 Academy of Sciences (the Program “Plasma Processes in the Solar System”).

References

- Berthelier, J. J., et al. (2006a), ICE, the electric field experiment on
 DEMETER, *Planet. Space Sci.*, 54, 456–471, doi:10.1016/j.
 pss.2005.10.016.
 Berthelier, J. J., et al. (2006b), IAP, the thermal plasma analyzer on
 DEMETER, *Planet. Space Sci.*, 54, 487–501, doi:10.1016/j.
 pss.2005.10.018.
 Carpenter, D. L., M. A. Spasojević, T. F. Bell, U. S. Inan, B. W. Reinisch,
 I. A. Galkin, R. F. Benson, J. L. Green, S. F. Fung, and S. A. Boardsen
 (2002), Small-scale field-aligned plasmaspheric density structures in-
 ferred from the Radio Plasma Imager on IMAGE, *J. Geophys. Res.*,
 107(A9), 1258, doi:10.1029/2001JA009199.
 Frolov, V. L., et al. (2008), Satellite measurements of plasma density pertur-
 bations induced in the topside ionosphere by high-power HF radio waves
 from the “SURA” heating facility, *Radiophys. Quantum Electron.*, 51(11),
 825–833.
 Gurevich, A. V., A. V. Lukyanov, and K. P. Zybin (1996), Anomalous
 absorption of powerful radio waves on the striations developed during
 ionospheric modification, *Phys. Lett. A*, 211, 363–372, doi:10.1016/
 0375-9601(95)00970-1.

- 337 Gustavsson, B., et al. (2001), First tomographic estimate of volume distri-
 338 bution of HF-pump enhanced airglow emission, *J. Geophys. Res.*, *106*
 339 (A12), 29,105–29,123, doi:10.1029/2000JA900167.
- 340 Huba, J. D., G. Joyce, and J. A. Fedder (2000), Sami2 is another model of the
 341 ionosphere (SAMI2): A new low-latitude ionosphere model, *J. Geophys.*
 342 *Res.*, *105*(A10), 23,035–23,053, doi:10.1029/2000JA000035.
- 343 Koons, H. C. (1989), Observations of large-amplitude, whistler-mode
 344 wave ducts in the outer plasmasphere, *J. Geophys. Res.*, *94*(A11),
 345 15,393–15,397, doi:10.1029/JA094iA11p15393.
- 346 Milikh, G. M., et al. (2008), Formation of artificial ionospheric ducts,
 347 *Geophys. Res. Lett.*, *35*, L17104, doi:10.1029/2008GL034630.
- 348 Perrine, R. P., G. M. Milikh, K. Papadopoulos, J. D. Huba, G. Joyce,
 349 M. Swisdak, and Y. Dimant (2006), An interhemispheric model of artifi-
 350 cial ionospheric ducts, *Radio Sci.*, *41*, RS4002, doi:10.1029/
 351 2005RS003371.
- 352 Rietveld, M. T., M. J. Kosch, N. F. Blagoveshchenskaya, V. A. Kormienko,
 353 T. B. Leyser, and T. K. Yeoman (2003), Ionospheric electron heating,
 optical emissions, and striations induced by powerful HF radio waves 354
 at high latitudes: Aspect angle dependence, *J. Geophys. Res.*, *108*(A4), 355
 1141, doi:10.1029/2002JA009543. 356
- Streltsov, A. V., M. Lampe, W. Manheimer, G. Ganguli, and G. Joyce 357
 (2006), Whistler propagation in inhomogeneous plasma, *J. Geophys.* 358
Res., *111*, A03216, doi:10.1029/2005JA011357. 359
-
- A. G. Demekhov, Institute of Applied Physics, Russian Academy of 360
 Sciences, 46 Ulyanov St., Nizhny Novgorod, 603950, Russia. 361
- J. D. Huba, Naval Research Laboratory, Washington, DC 20375-5320, 362
 USA. 363
- G. Joyce, Icarus Research, Inc., P.O. Box 30780, Bethesda, MD 20824- 364
 0780, USA. 365
- K. Papadopoulos, G. M. Milikh, and A. Vartanyan, Department of 366
 Astronomy, University of Maryland, College Park, MD 20742, USA. 367
 (milikh@astro.umd.edu) 368

Article in Proof